



Radiation Shielding Properties of Aluminosilicate Glass Systems using Phy-X Software

M. I. Sayyed^{1,*}

¹ Department of Physics, Faculty of Science, Isra University, 1162, Amman, Jordan

ARTICLE INFO

Article history:

Received 15 June 2023

Received in revised form 29 October 2023

Accepted 15 November 2023

Available online 16 January 2024

Keywords:

Aluminosilicate glasses; Phy-X software;
radiation shielding materials;
attenuation factors

ABSTRACT

In this work, we studied the radiation shielding properties of aluminosilicate glasses with constant SiO₂ content. By applying Phy-X software, we calculated different radiation attenuation factors for the chosen glasses. The linear attenuation coefficient (LAC) for the chosen CaO–Al₂O₃–SiO₂ glass systems showed an exponential decrease as the energy changes from 0.015 to 15 MeV. For the glass with composition of 35CaO–5Al₂O₃–60SiO₂, the LAC decreases from 29.80 to 1.279 cm⁻¹ between 0.015 and 0.05 MeV. The LAC decreases with the increase in the Al₂O₃ content. The minimum LAC is found for the glass with the composition of 20CaO–20Al₂O₃–60SiO₂. The effective atomic number (Z_{eff}) was reported, and we found that the highest Z_{eff} is occurred at 0.015 MeV and varied between 14.55 and 16.09. The Z_{eff} decreases when we replaced the CaO by Al₂O₃. The half value layer was reported and we discussed the impact of the density of the glasses on the HVL values. In the low energy range, the HVL values are small and the different compositions have close HVL. For E>0.08 MeV, the HVL is higher than 1 cm for all glasses, while for E> 0.2 MeV, the HVL becomes higher than 2 cm for all glasses. The glass with composition of 35CaO–5Al₂O₃–60SiO₂ has better attenuation performance than the other glasses in this study.

1. Introduction

Aluminosilicate glasses have excellent thermal and mechanical features, so they are used in different applications. One of these applications is the radiation shielding field. Radiation shielding materials are materials designed to attenuate the X-ray and gamma radiations or other types of radiation [1-3]. These materials are used to protect the human and environment from the hazard of the ionizing radiation. Lead and concrete are the two most popular materials used as radiation shields [4,5]. In addition, glasses in the current days are widely in the radiation shielding applications for many reasons. Glasses can be produced in different ways such as melt quenching method. Glasses are transparent materials, so we can use glasses in radiological rooms. We can easily modify the composition of the glasses in order to get effective glasses in radiation protection [6-8]. All these reasons encourage the researchers to develop glasses in radiation protection utilizations [9]. There

* Corresponding author.

E-mail address: dr.mabualssayed@gmail.com

<https://doi.org/10.37934/araset.37.2.156164>

are three methods to investigate the radiation shielding properties of the glasses: experimental method, theoretical method and simulation method [10]. In the experimental method, we need a suitable setup, which basically includes the samples, a detector, and the radioactive sources (such as Co-60, Cs-137 etc.). In the theoretical method, we use some basic equations and formulas to calculate some factors which describe the interactions between photons and the glasses. These factors are called attenuation factors. Some software can also be used to evaluate the attenuation factors such as WinXcoma and Phy-X software. In the simulation method we can use Monte Carlo simulation to simulate the interaction between the photons and the shield [11-15]. Using any of these previous methods, the researcher can determine the linear attenuation coefficient (LAC), the radiation protection efficiency (RPE) and other related factors. High LAC and RPE values for any glass are an indication of good radiation attenuation, so it is important to prepare glasses with high LAC and RPE values [16,17]. In contrast, a low half value layer is preferable in practical applications. In the literature, different research groups reported the LAC, RPE and other attenuation factors for borate, silicate, phosphate and other kinds of glasses [18]. In general, the previous works showed that one simplest way to enhance the radiation shielding performance is to use heavy metal oxides. Also, we can increase the thickness of the glass to get suitable radiation shielding materials [19,20]. In this work, we used theoretical method to study the radiation shielding properties of aluminosilicate glasses with constant SiO₂ content. Recently, there has been a growing attention in the development of new glass systems for gamma ray shielding utilizations. Glasses composed of SiO₂, Al₂O₃ and CaO have been investigated for their potential applications in different field. However, the majority of the previous works have focused on varying the concentration of SiO₂ in the glass composition, while in this study, we maintain a constant amount of SiO₂ content (60 mol%) and change the concentration of CaO and Al₂O₃. This allows us to isolate the impacts of Al₂O₃ and CaO on the gamma ray attenuation features of the glasses, giving new insights into the effect of these compounds in the attenuation of the photons.

2. Materials and Methods

In this work, we aimed to calculate the radiation shielding factors for aluminosilicate glasses with constant SiO₂ content. The selected glasses were previously prepared by Takahashi *et al.*, [21]. In their work, they reported the thermal and structural properties of these glasses. We extended this previous work, and evaluated the basic radiation shielding properties of these glasses. The following is the composition of the glasses:

- S1: 35CaO-5Al₂O₃-60SiO₂, density=2.73 g/cm³
- S2: 30CaO-10Al₂O₃-60SiO₂, density=2.69 g/cm³
- S3: 25CaO-15Al₂O₃-60SiO₂, density=2.65 g/cm³
- S4: 20CaO-20Al₂O₃-60SiO₂, density=2.62 g/cm³

For the determination of radiation attenuation factor, we used Phy-X software [22].

Phy-X software is highly useful in the radiation shielding field since we can determine the attenuation factors for any sample at different energy region. This software works by taking in the composition of the materials and their respective densities. The energy range desired can then be specified, using a general spectrum or specific radioisotopes that are commonly used in such testing. The needed factors are then chosen, which the software determines and provides as its output to be discussed

The linear attenuation coefficient (LAC or μ) is a basic factor in the radiation shielding study. The LAC can be determined using Lambert-Beer Law

$$I = I_0 e^{-\mu x} \quad (1)$$

where x is the thickness of the sample.

The half value layer is another useful shielding factor. It represents the thickness of the shielding materials in which I_0 changes to $0.5I_0$. We can use the next formula for the calculation of HVL

$$\text{HVL} = \frac{\ln(2)}{\text{LAC}} \quad (2)$$

The reciprocal of LAC is defined as the mean free path. Namely

$$\text{MFP} = \frac{1}{\text{LAC}} \quad (3)$$

The thickness of the materials needed to shield most of the incoming photons (i.e., I_0 becomes $0.1I_0$) is called the tenth value layer. Mathematically

$$\text{TVL} = \frac{\ln 10}{\text{LAC}} \quad (4)$$

By determining both the HVL and TVL values of a medium, radiation shielding designers can develop space-efficient shields.

The effective atomic number (Z_{eff}) of a material is calculated as

$$Z_{\text{eff}} = \frac{\sum_i f_i A_i \left(\frac{\mu}{\rho}\right)_i}{\sum_j f_j Z_j \left(\frac{\mu}{\rho}\right)_j} \quad (5)$$

Details about the attenuation factors can be found elsewhere [23-29].

3. Results and discussion

We plotted the linear attenuation coefficient (LAC) for the chosen $\text{CaO-Al}_2\text{O}_3\text{-SiO}_2$ glass systems with a constant amount of SiO_2 (60 mol%) in Figure 1. Apparently, the LAC values show an exponential decrease as the energy changes from 0.015 to 15 MeV. The rate of this decrease is very fast between 0.015 and 0.06 MeV, while it shows a slight decrease at higher energies. The quick decrease in LAC at the first few energies can be explained according to the dominance of the photoelectric effect. For example, for the glass with composition of $35\text{CaO-5Al}_2\text{O}_3\text{-60SiO}_2$, the LAC decreases from 29.80 to 1.279 cm^{-1} between 0.015 and 0.05 MeV. While, between 0.1 and 0.4 MeV, the LAC for the same sample is decreased only from 0.511 to 0.264 cm^{-1} . The trend in LAC at higher energies can be explained by Compton scattering and pair production. We can see from Figure 1 that the LAC decreases with the increase in the Al_2O_3 content. Since all glasses contain constant amount of SiO_2 (60 mol%), the increase in the Al_2O_3 content (or decrease in CaO content) causes a decrease in the density from 2.73 to 2.62 g/cm^3 which causes the reduction in the LAC due to the addition of Al_2O_3 . The minimum LAC is found for the glass with a composition of $20\text{CaO-20Al}_2\text{O}_3\text{-60SiO}_2$. The LAC for

this glass at 0.015, 0.03, 0.1, 0.5, 1 and 10 MeV are respectively 21.59, 3.143, 0.463, 0.228, 0.166 and 0.060 cm^{-1} .

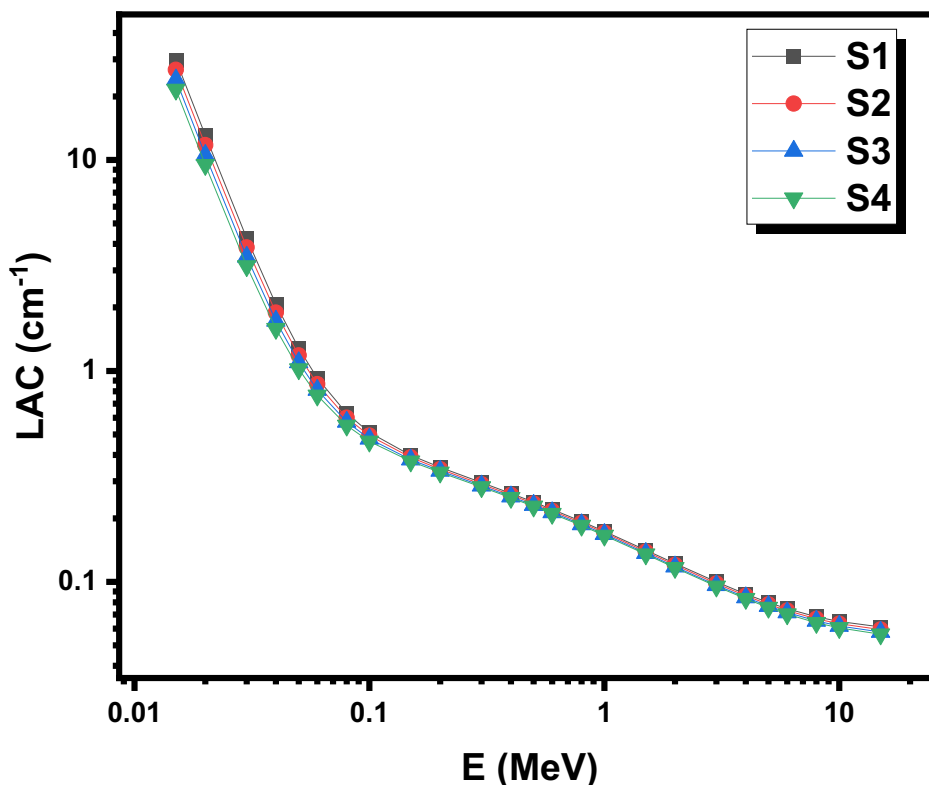


Fig. 1. The linear attenuation coefficient for the CaO–Al₂O₃–SiO₂ glass systems with constant amount of SiO₂ (60 mol%)

In Figure 2, we plotted the results of the effective atomic number (Z_{eff}) for the glasses with constant SiO₂ content. The highest Z_{eff} is found at 0.015 MeV and is equal to 16.09, 15.60, 15.09 and 14.55 for the S1 to S4 glasses respectively. The Z_{eff} at 0.02 MeV is in the order of 14.46-16.01 which is smaller than the Z_{eff} obtained at 0.015 MeV. Since the photoelectric effect is very important at low energy region, we can explain the highest Z_{eff} values for these glasses at low energy range. The Z_{eff} decreases with increasing the energy and reached the minimum values of 11.02 (for S1) and 10.50 (for S4). The minimum values of the effective atomic number at this energy can be explained according to Compton scattering. For $E > 1$ MeV, we found a slight increase in the Z_{eff} , where the Z_{eff} values for S1 and S4 are 11.71 and 11.00 at 15 MeV. Moreover, we can see that the concentration of CaO and Al₂O₃ is also affected the Z_{eff} . The Z_{eff} decreases when we replaced the CaO by Al₂O₃ and this is expected since the atomic number of Ca is higher than that of Al. For this reason, we found that the Z_{eff} decreases as we move from S1 to S4. Accordingly, the glass with a composition of 35CaO-5Al₂O₃-60SiO₂ has better attenuation performance than the other glasses in this study.

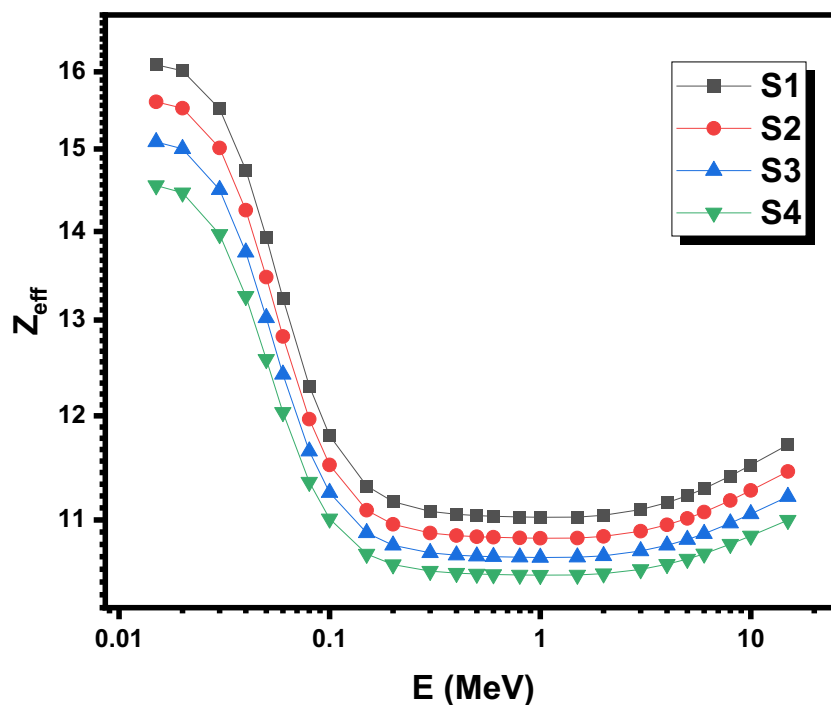


Fig. 2. The effective atomic number for the CaO–Al₂O₃–SiO₂ glass systems with constant amount of SiO₂ (60 mol%)

The half value layer for the chosen CaO–Al₂O₃–SiO₂ glass systems with constant amount of SiO₂ (60 mol%) is exhibited in Figure 3. In real utilizations, a smaller HVL is needed and we can get this by increasing the density of the sample. For the four selected glasses, the profile of HVL is similar, and this is expected since these glasses contain the same compounds, but the difference in the HVL between the samples is due to the change in the concentrations of CaO and Al₂O₃ between these glasses. For low energy, the HVL values are small and the different compositions have close HVL. Numerically, the HVL for the glasses with 5, 10, 15 and 20 mol% Al₂O₃ is 0.023, 0.026, 0.029 and 0.032 cm (this is at 0.015 MeV). For these glasses but at 0.03 MeV, the HVL values are 0.163, 0.180, 0.200 and 0.221 cm. For E>0.08 MeV, the HVL becomes higher than 1 cm for all glasses. Also, for E> 0.2 MeV, the HVL becomes higher than 2 cm for all glasses. While for E>0.5 MeV, the HVL for these glasses is higher than 3 cm. The maximum HVL is reported at 15 MeV and equals to 11.34, 11.66, 11.99 and 12.28 cm for the S1 to S4 glasses respectively. Moreover, S1 glass has a smaller HVL than S2-S4 glasses, while the highest HVL is found for S4. It is known that the HVL has an inverse relation with the density, so the S1 glass which possesses the highest density has a thinner HVL than the rest of the samples.

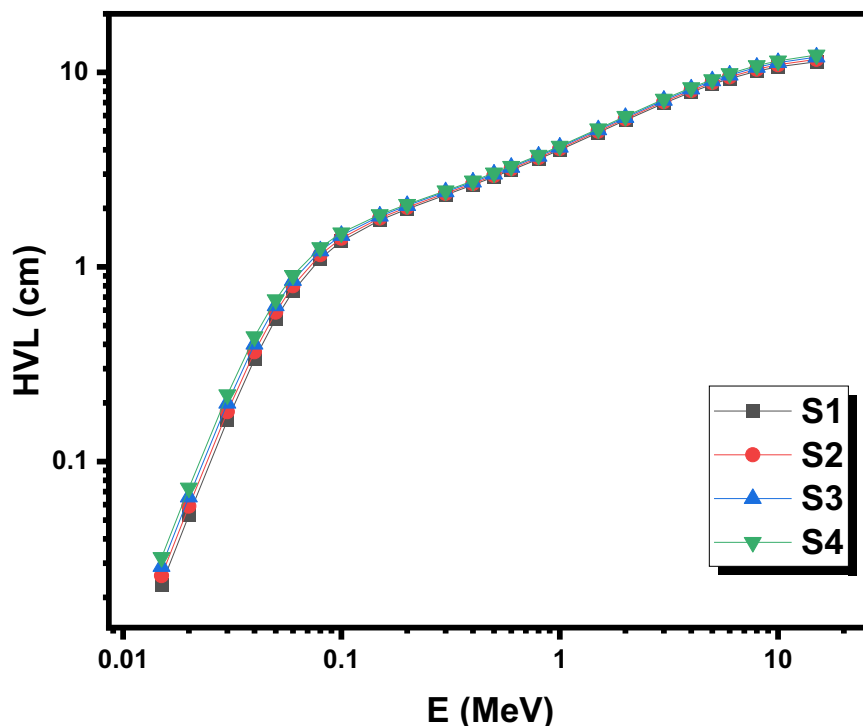


Fig. 3. The half value layer for the CaO–Al₂O₃–SiO₂ glass systems with constant amount of SiO₂ (60 mol%)

The tenth value layer values for the selected glasses at 0.1, 0.5 and 1 MeV were reported and presented in Figure 4. The TVL values increase as the energy increases from 0.1 to 1 MeV. This suggests that the thickness of the glasses must be increased to shield the photons with higher energies. Numerically, the TVL at 0.1 MeV is in the range of 4.97-4.5 cm, so we need a layer of thickness of around 5 cm in order to shield most of the incoming radiation with energy of 0.1 MeV. When it comes to radiation with energy of 0.5 MeV, we found that the TVL lies within the range of 9.64-10.09 cm. So, we need a thicker layer to block most of the radiation with energy of 0.5 MeV. The TVL for these glasses when the energy of the radiation is 1 MeV increases to 13.26-13.87 cm. So, the thickness of the glass is an important factor to be considered when we use the glasses in high energy radiation shielding applications.

The MFP is also determined and plotted in Figure 5. The MFP is small at the low energy range, ranging from 0.034 to 0.046 cm at 0.015 MeV, from 0.076 to 0.106 cm at 0.02 MeV and from 0.235 to 0.318 cm at 0.03 MeV. Thereafter, the MFP starts increasing and reaches to about 1 cm at 0.06 MeV. When the energy reached 0.1 MeV, we found that the MFP was on the order of 2 cm. With the increase in energy, the MFP continues to increase and reaches around 4 cm at 0.4 MeV. At 3 MeV, we found that the MFP is very high and equals to 10.01 cm for S1 and 10.52 cm for S2. The maximum MFP is determined at 15 MeV and equal to 16.36 cm for S1 and 17.71 cm for S4. Also, we found that the MFP increased with the addition of Al₂O₃. So, the sample with high Al₂O₃ content has high MFP. This is because the MFP has an inverse relation with the LAC, so when we added Al₂O₃, the LAC decreases and the MFP increases.

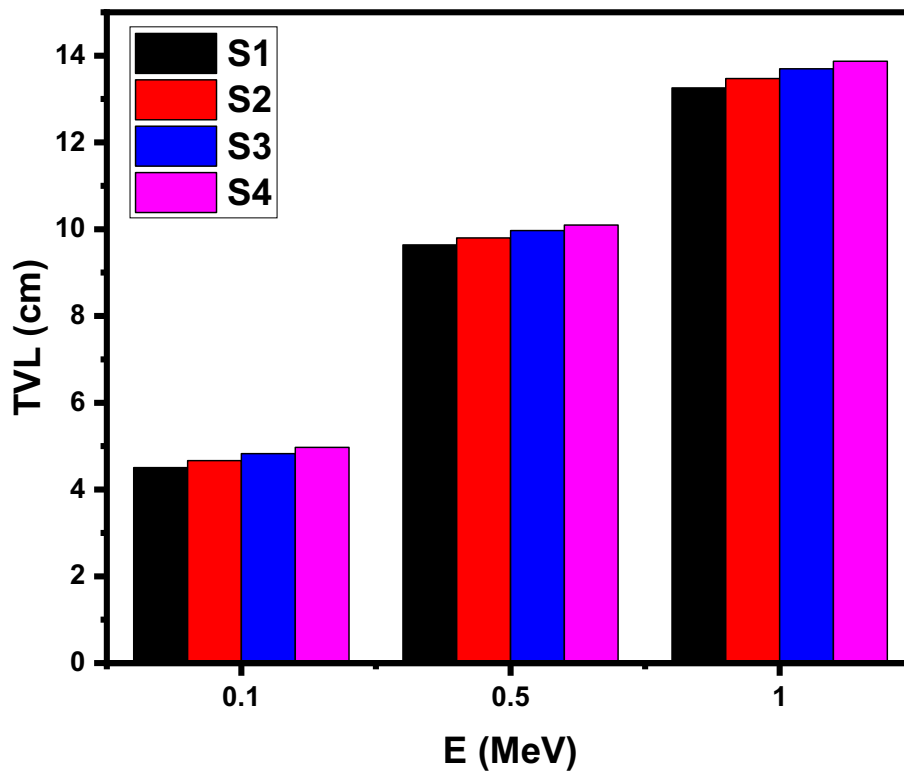


Fig. 4. The tenth value layer values for the selected glasses at 0.1, 0.5 and 1 MeV

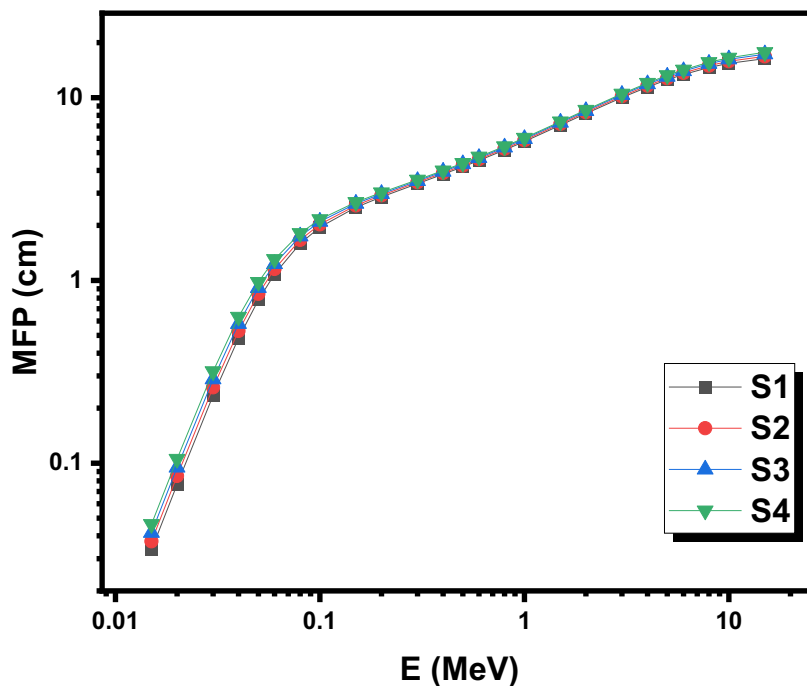


Fig. 5. The mean free path for the selected glasses at 0.1, 0.5 and 1 MeV

4. Conclusion

We reported the radiation attenuation parameters of aluminosilicate glasses with constant SiO₂ content with the help of Phy-X software. The LAC for the CaO–Al₂O₃–SiO₂ glass systems showed an exponential decrease with increasing the energy from 0.015 to 15 MeV. The maximum LAC is found for the glass with the composition of 35CaO-5Al₂O₃-60SiO₂. Also, this sample showed the highest Z_{eff} and the minimum HVL. The maximum Z_{eff} for the chosen glasses lies in the range of 14.55 and 16.09, while the minimum Z_{eff} is in the order of 10.50-11.02. We investigated the thickness of the glasses needed to shield 50% of the incoming photons and reported this thickness at different energy levels. At low energy, we found that the HVL is varied between 0.023 and 0.032 cm at 0.015 MeV. At 0.03 MeV, the HVL values are 0.163, 0.180, 0.200 and 0.221 cm. For E > 0.2 MeV, the HVL becomes higher than 2 cm for all glasses. Also, for E > 0.5 MeV, the HVL for these glasses is higher than 3 cm. The maximum HVL is reported at 15 MeV and equal to 11.34, 11.66, 11.99 and 12.28 cm for the S1 to S4 glasses

Acknowledgement

This research was not funded by any grant.

References

- [1] Prasad, Rishu, Avinash R. Pai, S. Olutunde Oyadiji, Sabu Thomas, and S. K. S. Parashar. "Utilization of hazardous red mud in silicone rubber/MWCNT nanocomposites for high performance electromagnetic interference shielding." *Journal of Cleaner Production* 377 (2022): 134290. <https://doi.org/10.1016/j.jclepro.2022.134290>
- [2] Özdemir, Tonguç, and Seda Nur Yılmaz. "Mixed radiation shielding via 3-layered polydimethylsiloxane rubber composite containing hexagonal boron nitride, boron (III) oxide, bismuth (III) oxide for each layer." *Radiation Physics and Chemistry* 152 (2018): 17-22. <https://doi.org/10.1016/j.radphyschem.2018.07.007>
- [3] Sayyed, M. I. "The role of Bi₂O₃ on radiation shielding characteristics of ternary bismuth tellurite glasses." *Optik* 270 (2022): 169973. <https://doi.org/10.1016/j.ijleo.2022.169973>
- [4] Naseer, K. A., K. Marimuthu, K. A. Mahmoud, and M. I. Sayyed. "Impact of Bi₂O₃ modifier concentration on barium–zincborate glasses: physical, structural, elastic, and radiation-shielding properties." *The European Physical Journal Plus* 136 (2021): 1-23. <https://doi.org/10.1140/epjp/s13360-020-01056-6>
- [5] Kim, Seulgi, Yunhee Ahn, Sung Ho Song, and Dongju Lee. "Tungsten nanoparticle anchoring on boron nitride nanosheet-based polymer nanocomposites for complex radiation shielding." *Composites Science and Technology* 221 (2022): 109353. <https://doi.org/10.1016/j.compscitech.2022.109353>
- [6] Saleh, Abdelmoneim. "Comparative shielding features for X/Gamma-rays, fast and thermal neutrons of some gadolinium silicoborate glasses." *Progress in Nuclear Energy* 154 (2022): 104482. <https://doi.org/10.1016/j.pnucene.2022.104482>
- [7] Abualsayed, Mohammad Ibrahim. "Radiation attenuation attributes for BaO-TiO₂-SiO₂-GeO₂ glass series: a comprehensive study using Phy-X software." *Radiochimica Acta* 111, no. 3 (2023): 211-216. <https://doi.org/10.1515/ract-2022-0095>
- [8] Bagheri, Reza, Alireza Khorrami Moghaddam, and Hassan Yousefnia. "Gamma ray shielding study of barium–bismuth–borosilicate glasses as transparent shielding materials using MCNP-4C code, XCOM program, and available experimental data." *Nuclear Engineering and Technology* 49, no. 1 (2017): 216-223. <https://doi.org/10.1016/j.net.2016.08.013>
- [9] Acikgoz, Abuzer, Gokhan Demircan, Demet Yılmaz, Bulent Aktas, Serife Yalcin, and Nuri Yorulmaz. "Structural, mechanical, radiation shielding properties and albedo parameters of alumina borate glasses: Role of CeO₂ and Er₂O₃." *Materials Science and Engineering: B* 276 (2022): 115519. <https://doi.org/10.1016/j.mseb.2021.115519>
- [10] Kamislioglu, M. "An investigation into gamma radiation shielding parameters of the (Al: Si) and (Al+ Na): Si-doped international simple glasses (ISG) used in nuclear waste management, deploying Phy-X/PSD and SRIM software." *Journal of Materials Science: Materials in Electronics* 32 (2021): 12690-12704. <https://doi.org/10.1007/s10854-021-05904-8>
- [11] Kamislioglu, M. "Research on the effects of bismuth borate glass system on nuclear radiation shielding parameters." *Results in Physics* 22 (2021): 103844. <https://doi.org/10.1016/j.rinp.2021.103844>

- [12] Sayyed, M. I., Kawa M. Kaky, Erdem Şakar, Uğur Akbaba, Malaa M. Taki, and O. Agar. "Gamma radiation shielding investigations for selected germanate glasses." *Journal of Non-Crystalline Solids* 512 (2019): 33-40. <https://doi.org/10.1016/j.jnoncrysol.2019.02.014>
- [13] Zubair, Muhammad, Eslam Ahmed, and Donny Hartanto. "Comparison of different glass materials to protect the operators from gamma-rays in the PET using MCNP code." *Radiation Physics and Chemistry* 190 (2022): 109818. <https://doi.org/10.1016/j.radphyschem.2021.109818>
- [14] Sharma, Amandeep, M. I. Sayyed, O. Agar, and H. O. Tekin. "Simulation of shielding parameters for TeO₂-WO₃-GeO₂ glasses using FLUKA code." *Results in Physics* 13 (2019): 102199. <https://doi.org/10.1016/j.rinp.2019.102199>
- [15] Geidam, I. G., K. A. Matori, M. K. Halimah, K. T. Chan, F. D. Muhammad, M. Ishak, and S. A. Umar. "Oxide ion polarizabilities and gamma radiation shielding features of TeO₂-B₂O₃-SiO₂ glasses containing Bi₂O₃ using Phy-X/PSD software." *Materials Today Communications* 31 (2022): 103472. <https://doi.org/10.1016/j.mtcomm.2022.103472>
- [16] Sayyed, M. I., Mohammad Hasan Abu Mhareb, Y. S. M. Alajerami, K. A. Mahmoud, Mohammad A. Imheidat, Fatimh Alshahri, Muna Alqahtani, and T. Al-Abdullah. "Optical and radiation shielding features for a new series of borate glass samples." *Optik* 239 (2021): 166790. <https://doi.org/10.1016/j.jilleo.2021.166790>
- [17] Aktas, Bulent, Abuzer Acikgoz, Demet Yilmaz, Serife Yalcin, Kaan Dogru, and Nuri Yorulmaz. "The role of TeO₂ insertion on the radiation shielding, structural and physical properties of borosilicate glasses." *Journal of Nuclear Materials* 563 (2022): 153619. <https://doi.org/10.1016/j.jnucmat.2022.153619>
- [18] Issa, Shams AM, Ashok Kumar, M. I. Sayyed, M. G. Dong, and Y. Elmahroug. "Mechanical and gamma-ray shielding properties of TeO₂-ZnO-NiO glasses." *Materials Chemistry and Physics* 212 (2018): 12-20. <https://doi.org/10.1016/j.matchemphys.2018.01.058>
- [19] Kozlovskiy, A. L., and M. V. Zdorovets. "Effect of doping of Ce⁴⁺/3+ on optical, strength and shielding properties of (0.5-x) TeO₂-0.25 MoO₃-0.25 Bi₂O₃-xCeO₂ glasses." *Materials Chemistry and Physics* 263 (2021): 124444. <https://doi.org/10.1016/j.matchemphys.2021.124444>
- [20] Akçalı, Özgür, Mustafa Çağlar, Ozan Toker, Bayram Bilmez, H. Birtan Kavanoz, and Orhan İçelli. "An investigation on gamma-ray shielding properties of quaternary glassy composite (Na₂Si₃O₇/Bi₂O₃/B₂O₃/Sb₂O₃) by BXCUM and MCNP 6.2 code." *Progress in Nuclear Energy* 125 (2020): 103364. <https://doi.org/10.1016/j.pnucene.2020.103364>
- [21] Takahashi, Shoji, Daniel R. Neuville, and Hiromichi Takebe. "Thermal properties, density and structure of percalcic and peraluminous CaO-Al₂O₃-SiO₂ glasses." *Journal of Non-Crystalline Solids* 411 (2015): 5-12. <https://doi.org/10.1016/j.jnoncrysol.2014.12.019>
- [22] Şakar, Erdem, Özgür Fırat Özpolat, Bünyamin Alım, M. I. Sayyed, and Murat Kurudirek. "Phy-X/PSD: development of a user friendly online software for calculation of parameters relevant to radiation shielding and dosimetry." *Radiation Physics and Chemistry* 166 (2020): 108496. <https://doi.org/10.1016/j.radphyschem.2019.108496>
- [23] Aygün, Bünyamin. "High alloyed new stainless steel shielding material for gamma and fast neutron radiation." *Nuclear Engineering and Technology* 52, no. 3 (2020): 647-653. <https://doi.org/10.1016/j.net.2019.08.017>
- [24] Aygün, Bünyamin. "Neutron and gamma radiation shielding Ni based new type super alloys development and production by Monte Carlo Simulation technique." *Radiation Physics and Chemistry* 188 (2021): 109630. <https://doi.org/10.1016/j.radphyschem.2021.109630>
- [25] Bilici, Sevim, Mirac Kamislioglu, and Elif Ebru Altunsoy Guclu. "A Monte Carlo simulation study on the evaluation of radiation protection properties of spectacle lens materials." *The European Physical Journal Plus* 138, no. 1 (2023): 80. <https://doi.org/10.1140/epjp/s13360-022-03579-6>
- [26] Tekin, H. O., M. I. Sayyed, E. E. Altunsoy, and T. Manici. "Shielding properties and effects of WO₃ and PbO on mass attenuation coefficients by using MCNPX code." *Dig. J. Nanomater. Biostruct* 12, no. 3 (2017): 861-867.
- [27] Abualsayed, Mohammad Ibrahim, and Nouf Almousa. "Effect of tungsten on radiation attenuation features of γ WO₃-(90-γ) TeO₂-10Na₂O glasses." *Radiochimica Acta* 111, no. 3 (2023): 225-230. <https://doi.org/10.1515/ract-2022-0101>
- [28] Saleh, Abdelmoneim, M. G. El-Feky, M. S. Hafiz, and N. A. Kawady. "Experimental and theoretical investigation on physical, structure and protection features of TeO₂-B₂O₃ glass doped with PbO in terms of gamma, neutron, proton and alpha particles." *Radiation Physics and Chemistry* 202 (2023): 110586. <https://doi.org/10.1016/j.radphyschem.2022.110586>
- [29] Shahboub, A., G. El Damrawi, and A. Saleh. "A new focus on the role of iron oxide in enhancing the structure and shielding properties of Ag₂O-P₂O₅ glasses." *The European Physical Journal Plus* 136 (2021): 1-17. <https://doi.org/10.1140/epjp/s13360-021-01948-1>